Electronic Supplementary Material (ESI) for Chemical Science.
This journal is © The Royal Society of Chemistry 2014

Selective Label-Free Detection of G-Quadruplex Structure of Human Telomere by Emission Spectral Changes in Visible-and-NIR Region under Physiological Condition through the FRET of a Two-Component PPE-SO_3^-–Pt(II) Complex Ensemble with Pt···Pt, Electrostatic and π–π Interactions

*Clive Yik-Sham Chung and Vivian Wing-Wah Yam**

Institute of Molecular Functional Materials, (Area of Excellence Scheme, University Grants Committee, Hong Kong) and Department of Chemistry, The University of Hong Kong, Pokfulam Road, Hong Kong, P. R. China

*To whom correspondence should be addressed. Email: wwyam@hku.hk

Supporting Information

Experimental Section

Materials and Reagents. 2-Acetylpyridine, *p*-tolualdehyde, 2,2′-azobis(2-methyl-propionitrile) (AIBN), 4-iodotoluene, 1-*tert*-butyl-4-iodobenzene, methyl 4-iodobenzoate and ethyl 4-iodobenzoate were purchased from Sigma-Aldrich. 4'-(*p*-Tolyl)-2,2':6',2''-terpyridine,[S1] 4'-(4-(bromomethyl)phenyl)-2,2':6',2''-terpyridine,[S2] 4-trimethylsilylethynyltoluene,[S3] 4-ethynyltoluene,[S3] 1-*tert*-butyl-4-(2'-trimethylsilylethynyl)benzene,[S4] 1-*tert*-butyl-4-ethynylbenzene[S4] and 1-ethynyl-3,5-dimethoxybenzene[S5] were synthesized according to the reported literature methods. Human serum albumin (HSA), lysozyme, trypsin, poly(tyrosine) (M_w=10,000-40,000) and spermine were purchased from Sigma-Aldrich. Human telomeric DNA (5'-TTAGGGTTAGGGTTAGGGTTAGGGTTA-3'), *bcl-2* (5'-GGG-CGCGGGAGGAAGGGGGCGGG-3'), *c-kit* (5'-AGGGAGGGCGCTGGGAGGA-GGG-3'), *c-myc* (5'-TGAGGGTGGGGAGGGTGGGGAA-3') and other poly(nucleotides) were obtained from Sigma-Proligo (St. Louis, MO). Poly(sodium *p*-styrenesulfonate) (M_w ~70,000) was purchased from Acros. All other reagents were of analytical grade and were used without further purification. The reactions were performed under an inert atmosphere of nitrogen unless specified otherwise.

Physical Measurements and Instrumentation. ^{1}H NMR spectra were recorded with a Bruker AVANCE 400 (400 MHz) Fourier transform NMR spectrometer at ambient temperature with tetramethylsilane (Me_4Si) as an internal reference. Positive ion FAB or EI mass spectra were recorded on a Thermo Scientific DFS High Resolution Magnetic Sector mass spectrometer. Elemental analyses for the metal complexes were performed on the Carlo Erba 1106 elemental analyzer at the Institute of Chemistry, Chinese Academy of Sciences, Beijing, China. IR spectra of the solid samples were obtained as KBr disks on a Bio-Rad FTS-7 Fourier transform infrared

spectrophotometer (4000-400 cm^{-1}). UV-Vis absorption spectra were recorded on a Cary 50 (Varian) spectrophotometer equipped with a Xenon flash lamp. Steady state emission spectra were recorded using a Spex Fluorolog-3 Model FL3-211 fluorescence spectrofluorometer equipped with a R2658P PMT detector. Time-resolved emission decay profiles were recorded with a Horiba Jobin Yvon FluoroCube based on a time-correlated single photon counting method, using a nanoLED with peak wavelength and pulse duration equal to 371 nm and < 200 ps respectively as the excitation source. Unless specified otherwise, the emission spectra were corrected for PMT response. Resonance light scattering (RLS) experiments were performed on Spex Fluorolog-3 Model FL3-211 fluorescence spectrofluorometer with a Xenon flash lamp using a right-angle geometry to a R2658P PMT detector. The excitation and emission monochromator wavelengths were coupled and adjusted to scan simultaneously through the range of 350 to 600 nm.

Synthesis of PPE-SO_3^-. The polymer was synthesized according to the method reported in the literature.[S6] Its purity was confirmed by ^{1}H NMR and the molecular weight was estimated to be 150 kD based on its ultrafiltration properties. ^{1}H NMR (400 MHz, DMSO-d_6, 353 K): δ = 2.12 (br, 4H), 2.71 (br, 4H), 4.14 (br, 4H), 7.17 (br, 2H), 7.76 (br, 4H).

Synthesis of 4'-(4-(Trimethylamino)methylphenyl)-2,2':6',2''-terpyridine trifluoromethanesulfonate ([L][OTf]). 4'-(4-(Trimethylamino)methylphenyl)-2,2':6',2''-terpyridine bromide was synthesized according to the reported literature.[S7] Metathesis reaction of the bromide salt (800 mg, 1.73 mmol) with AgOTf gave the trifluoromethanesulfonate salt as an off-white solid. Yield = 600 mg (65%). ^{1}H NMR (300 MHz, MeOD-d_4): δ = 3.20 (s, 9H), 4.67 (s, 2H), 7.36 (m, 2H), 7.84 (d, *J* = 8.3

Hz, 2H), 8.01 (m, 2H), 8.10-8.13 (m, 2 H), 8.18 (d, *J* = 8.3 Hz, 2H), 8.37 (d, *J* = 8.0 Hz, 2H), 8.54 (s, 2H). Positive FAB-MS, *m/z*: 531. Elemental analysis calcd (%) for $C_{26}H_{25}F_3N_4O_3S$: C 58.86, H 4.75, N 10.56; found: C 58.79, H 5.01, N 10.18.

Synthesis of [Pt(L)Cl](OTf)$_2$. This was synthesized according to modification of a literature procedure for [Pt(tpy)Cl](OTf)[S8] using [L][OTf] (219 mg, 0.41 mmol) instead of tpy. Yield = 300 mg (80 %). ^{1}H NMR (400 MHz, DMSO-d$_6$): δ = 3.10(s, 9H), 4.64 (s, 2H), 7.85 (d, *J* = 8.3 Hz, 2H), 8.02 (m, 2H), 8.36 (d, *J* = 8.3 Hz, 2H), 8.60-8.62 (m, 2H), 8.89 (d, *J* = 8.3 Hz, 2H), 9.02 (d, *J* = 4.8 Hz, 2H), 9.09 (s, 2H). Positive FAB-MS, *m/z*: 761 $[M - OTf]^+$. Elemental analysis calcd (%) for $C_{27}H_{25}ClF_6N_4O_6PtS_2 \bullet H_2O$: C 34.94, H 2.93, N 6.04; found: C 35.21, H 2.95, N 6.05.

Synthesis of complex 1. The ligand [H-C≡C$C_6H_4CH_2NMe_3$-4](OTf) and complex **1** were synthesized as reported previously.[S9]

Synthesis of complex 2. Complex **2** was synthesized by dehydrohalogenation reaction of [Pt(L)Cl](OTf)$_2$ (300 mg, 0.33 mmol) and phenylacetylene (102 mg, 1 mmol) in the presence of CuI (6 mg, 0.03 mmol) as the catalyst in DMF (10 mL) and distilled triethylamine (1 mL).[S10] After an overnight reaction, the solvent was distilled out under vacuum. The crude product was dissolved in methanol-acetonitrile mixture and any undissolved solid was filtered off. The filtrate was evaporated under reduced pressure. Subsequent recrystallization by diffusion of diethyl ether vapour into the methanol-acetonitrile solution of **2** gave the product as a red-orange solid. Yield = 120 mg (37 %). ^{1}H NMR (400 MHz, DMSO-d$_6$, 353 K): δ = 3.10 (s, 9H), 4.67 (s, 2H), 7.30 (m, 1H), 7.36 (m, 2H), 7.52 (d, *J* = 5.3 Hz, 2H), 7.82 (d, *J* = 8.3 Hz, 2H), 8.02 (m, 2H), 8.33 (d, *J* = 8.3 Hz, 2H), 8.57 (m, 2H), 8.84 (d, *J* = 8.3 Hz, 2H), 9.10 (s, 2H),

9.29 (d, J = 4.8 Hz, 2H). IR (KBr disk, ν/cm^{-1}): 2120 (w, C≡C), 1164 (s, S=O). Positive FAB-MS, *m/z*: 826 [M – OTf]$^+$. Elemental analysis calcd (%) for $C_{35}H_{30}F_6N_4O_6PtS_2$•$CHCl_3$: C 39.48, H 2.85, N 5.12; found: C 39.16, H 2.97, N 5.39.

Synthesis of complex 3. The procedure was similar to that for complex **2** except that 4-ethynyltoluene (116 mg, 1 mmol) was used instead of phenylacetylene. The product was obtained as a dark red solid. Yield = 150 mg (46 %). ^{1}H NMR (400 MHz, DMSO-d_6, 353 K): δ = 2.33 (s, 3H), 3.13 (s, 9H), 4.68 (s, 2H), 7.18 (d, J = 7.8 Hz, 2H), 7.42 (d, J = 7.8 Hz, 2H), 7.81 (d, J = 8.3 Hz, 2H), 7.99 (m, 2H), 8.32 (d, J = 8.3 Hz, 2H), 8.57 (m, 2H), 8.86 (d, J = 8.3 Hz, 2H), 9.05 (s, 2H), 9.30 (d, J = 4.8 Hz, 2H). IR (KBr disk, ν/cm^{-1}): 2119 (w, C≡C), 1166 (s, S=O). Positive FAB-MS, *m/z*: 840 [M – OTf]$^+$. Elemental analysis calcd (%) for $C_{36}H_{32}F_6N_4O_6PtS_2$•$CH_2Cl_2$: C 41.35, H 3.19, N 5.21; found: C 41.60, H 3.25, N 5.36.

Synthesis of complex 4. The procedure was similar to that for complex **2** except that 1-*tert*-butyl-4-ethynylbenzene (158 mg, 1 mmol) was used instead of phenylacetylene. The product was obtained as a dark red solid. Yield = 140 mg (41 %). ^{1}H NMR (400 MHz, DMSO-d_6, 353 K): δ = 1.33 (s, 9H), 3.15 (s, 9H), 4.68 (s, 2H), 7.38 (d, J = 7.8 Hz, 2H), 7.45 (d, J = 7.8 Hz, 2H), 7.86 (d, J = 8.3 Hz, 2H), 8.00 (m, 2H), 8.33 (d, J = 8.3 Hz, 2H), 8.57 (m, 2H), 8.86 (d, J = 8.3 Hz, 2H), 9.05 (s, 2H), 9.29 (d, J = 4.8 Hz, 2H). IR (KBr disk, ν/cm^{-1}): 2119 (w, C≡C), 1170 (s, S=O). Positive FAB-MS, *m/z*: 882 [M – OTf]$^+$. Elemental analysis calcd (%) for $C_{39}H_{38}F_6N_4O_6PtS_2$: C 45.39, H 3.71, N 5.43; found: C 45.64, H 3.68, N 5.05.

Synthesis of complex 5. The procedure was similar to that for complex **2** except that 1-ethynyl-3,5-dimethoxybenzene (178 mg, 1.0 mmol) was used instead of

1,3-dihydroxy-5-trimethylsilylethynylbenzene. The product was obtained as a dark red solid. Yield = 140 mg (41%). ^{1}H NMR (400 MHz, DMSO-d_6, 353 K): δ = 3.23 (s, 9H), 3.80 (s, 6H), 4.68 (s, 2H), 6.46 (s, 1H), 6.71 (s, 2H), 7.87 (d, *J* = 8.2 Hz, 2H), 8.00 (m, 2H), 8.31 (d, *J* = 7.8 Hz, 2H), 8.55 (m, 2H), 8.86 (d, *J* = 7.8 Hz, 2H), 9.05 (s, 2H), 9.29 (d, *J* = 5.0 Hz, 2H). IR (KBr disk, ν/cm^{-1}): 2106 (w, C≡C), 1257 (s, C—O), 1157 (s, S=O). Positive FAB-MS, *m/z*: 887 [M – OTf]$^+$. Elemental analysis calcd (%) for $C_{37}H_{34}F_6N_4O_8PtS_2$•EtOH: C 43.29, H 3.73, N 5.18; found: C 43.24, H 3.73, N 4.89.

Preparation of G-quadruplex and duplex DNA.[S11] In order to ensure the formation of the G-quadruplex structure, the respective human telomeric DNA, *bcl-2*, *c-kit* or *c-myc* were dissolved in the aqueous buffer solution (50 mM KH_2PO_4, pH 6.8) with the desired concentration. The solution was heated at 95 ^{o}C for 5 minutes, cooled slowly to room temperature and then incubated at room temperature overnight.

The duplex DNA was prepared similarly by mixing two complementary poly(nucleotides) (Poly(dA)$_{25}$ and Poly(dT)$_{25}$; Poly(dG)$_{25}$ and Poly(dC)$_{25}$) in the aqueous buffer solution (50 mM KH_2PO_4, pH 6.8) with the desired concentration. The solution was heated at 95 ^{o}C for 5 minutes, cooled slowly to room temperature and then incubated at room temperature overnight.

Determination of Förster radius, R_0, of platinum(II) complexes with PPE-SO_3^-. R_0 was calculated from the equation $R_0 = 0.211[\kappa^2 n^{-4} \Phi_D J(\lambda)]^{1/6}$,[S12] where κ accounts for the relative orientation of the transition dipoles of the two chromophores (κ^2 is equal to 2/3 for randomly oriented dipoles), *n* is the refractive index of the solvent system, Φ_D is the emission quantum yield of PPE-SO_3^- donor in the aqueous buffer solution (30 mM Tris-HCl, 30 mM NaCl, pH 9.0) which was found to be 0.05 with

reference to quinine sulfate in 0.5 M H_2SO_4 at room temperature, $J(\lambda)$ is the donor-acceptor spectral overlap integral where the absorption spectra of the aggregated platinum(II) complexes were recorded using poly(sodium *p*-styrenesulfonate) instead of PPE-SO_3^- in order to minimize the interference from the absorption of the conjugated polymer.

Determination of binding constants of the PPE-SO_3^-−2 ensemble or complex 2 with human telomeric DNA and duplex DNA. The PPE-SO_3^-−**2** ensemble (concentration of PE-SO_3^- and **2** were both 45 μM) or complex **2** (45 μM) in aqueous buffer solution (50 mM KH_2PO_4, pH 6.8) was titrated with different concentrations of DNAs. The binding constants of the ensemble or complex **2** on the DNAs, *K*, were determined from the Scatchard equation,[S13] which states that:

$$D/\Delta\varepsilon_{app} = D/\Delta\varepsilon + 1/[(\Delta\varepsilon)K]$$

where *D* is the concentration of the base pairs of human telomeric DNA, $\Delta\varepsilon_{app} = [\varepsilon_A - \varepsilon_F]$ and $\Delta\varepsilon = [\varepsilon_B - \varepsilon_F]$. ε_A is calculated from the observed absorbance divided by the concentration of PPE-SO_3^-−**2** ensemble (45 μM) or complex **2** (45 μM), while ε_B and ε_F correspond to the molar extinction coefficients of the DNA−ensemble adduct or DNA−**2** adduct, and the unbound ensemble or complex **2** respectively.

By the plot of $D/\Delta\varepsilon_{app}$ against *D*, $\Delta\varepsilon$ and *K* can be found from the slope and the y-intercept of the graph respectively.

UV melting study of the PPE-SO_3^-−2 ensemble on human telomeric DNA.[S14] The electronic absorption spectra of human telomeric DNA (30 μM) in aqueous buffer solution (50 mM KH_2PO_4, pH 6.8) in the absence and in the presence of PPE-SO_3^-−**2** ensemble (concentration of PE-SO_3^- and **2** in the final solution mixture were both 30 μM) was monitored at different temperatures respectively. The melting temperature of

the G-quadruplex structure of human telomeric DNA, T_m, was determined graphically from the plots of absorbance against temperature. The absorption changes were monitored at 212 and 258 nm, which are the isosbestic point in the absorption spectra of the ensemble at different temperatures and the selected wavelength for UV melting study commonly employed in the literature, respectively.[S14b]

UV melting study of complex 2 on human telomeric DNA, *bcl-2*, *c-kit* or *c-myc*.[S14]

The electronic absorption spectra of human telomeric DNA, *bcl-2*, *c-kit* and *c-myc* (4 μM) in aqueous buffer solution (50 mM KH_2PO_4, pH 6.8) in the absence and in the presence of complex **2** (4 μM) were monitored at different temperatures respectively. The melting temperatures of the G-quadruplex structures, T_m, were determined graphically from the plots of absorbance against temperature.[S14b]

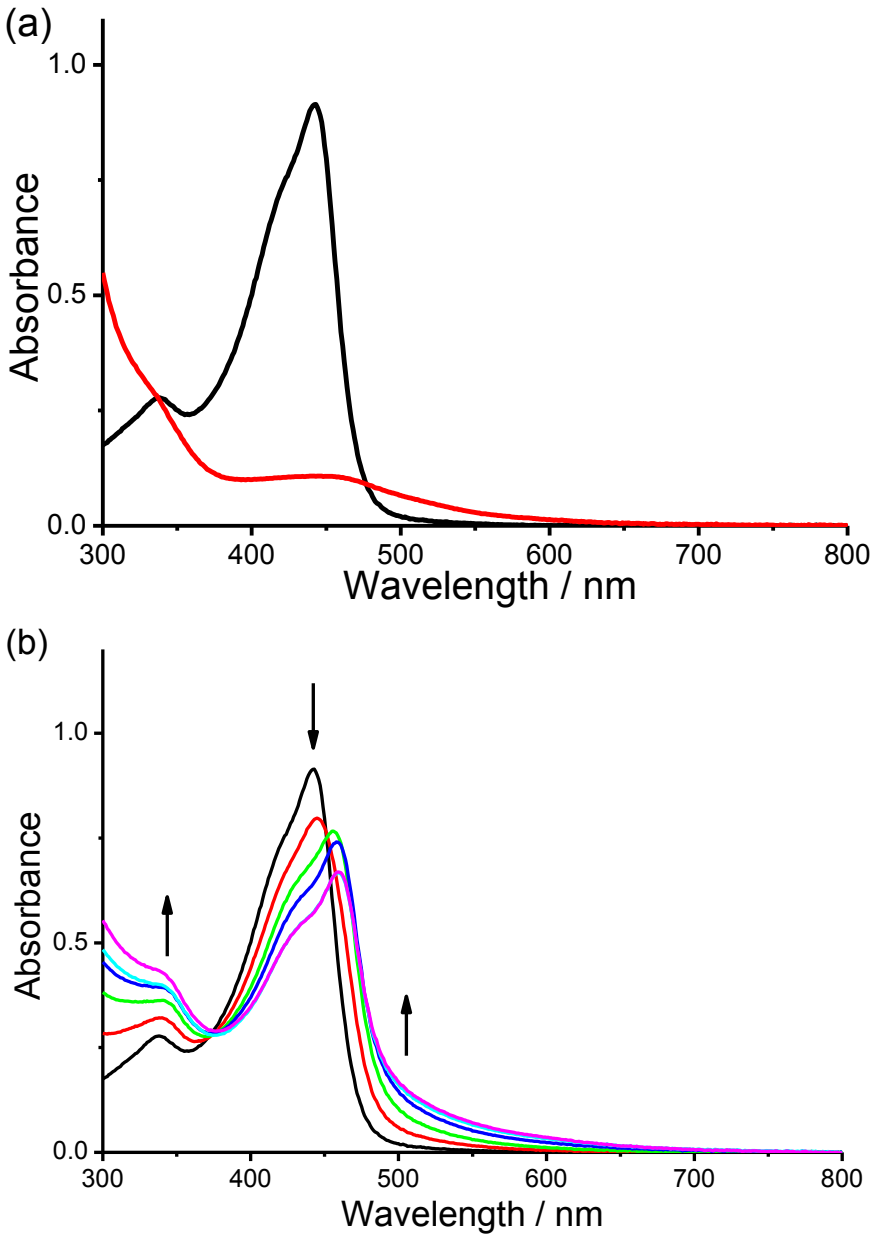

Fig. S1 (a) Electronic absorption spectra of PPE-SO_3^- (black) and complex **2** (red) in an aqueous buffer solution (30 mM Tris-HCl, 30 mM NaCl, pH 9.0). Concentration of **2** and sulfonate groups in PPE-SO_3^- (PE-SO_3^-) were both 45 μM. (b) Electronic absorption spectral changes of PPE-SO_3^- in the aqueous buffer solution with an increasing concentration of **2.** Concentration of PE-SO_3^- was 45 μM and that of **2** was 0 μM (black), 7.5 μM (red), 15 μM (green), 22.5 μM (blue), 30 μM (cyan), 45 μM (magenta) respectively.

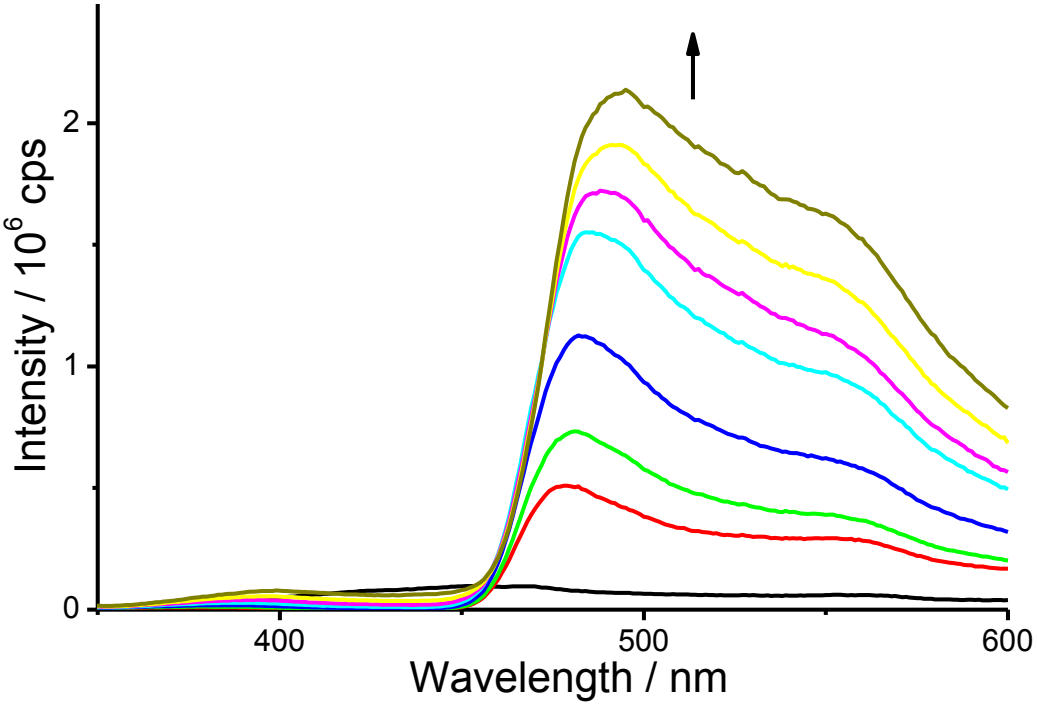

Fig. S2 Resonance light scattering (RLS) spectra of PPE-SO_3^- in an aqueous buffer solution (30 mM Tris-HCl, 30 mM NaCl, pH 9.0) with different concentrations of **2**. Concentration of PE-SO_3^- was 45 μM and that of **2** was 0 μM (red), 7.5 μM (green), 15 μM (blue), 22.5 μM (cyan), 30 μM (magenta), 37.5 μM (yellow) and 45 μM (dark yellow) respectively. The black line represents the signal of aqueous buffer solution (30 mM Tris-HCl, 30 mM NaCl, pH 9.0).

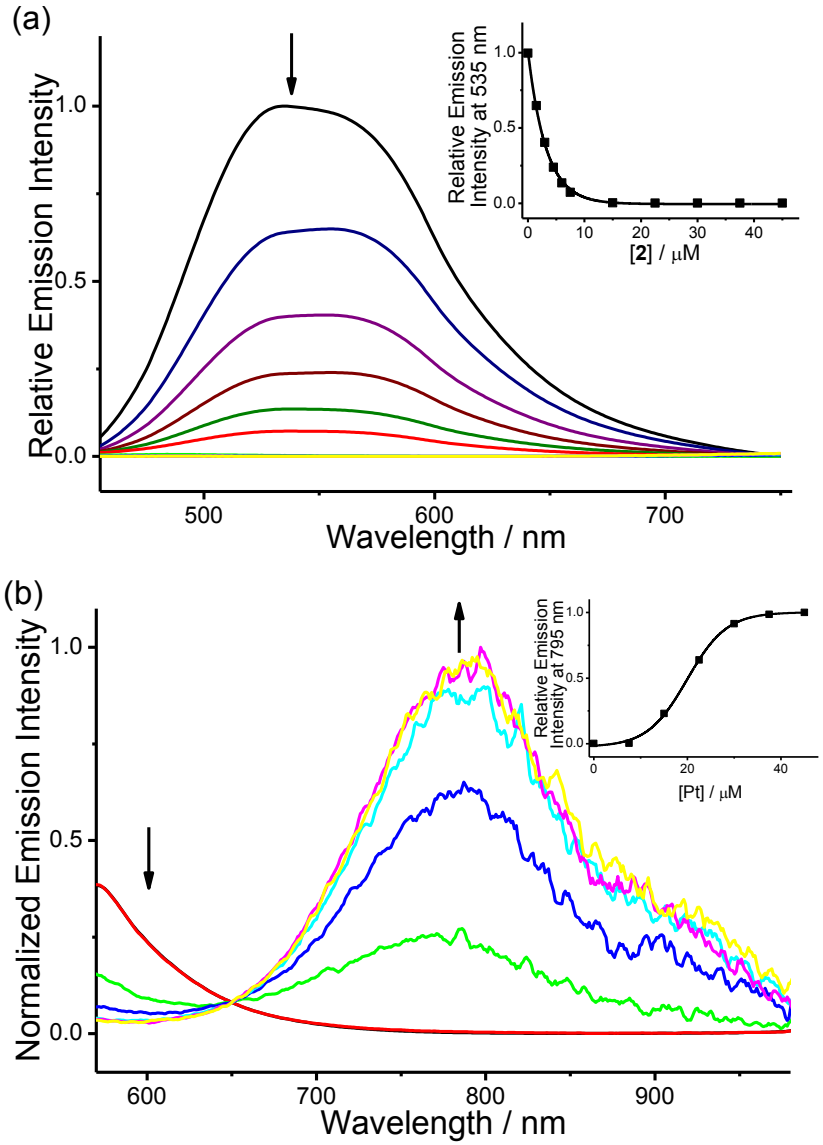

Fig. S3 Emission spectral changes of PPE-SO_3^- in an aqueous buffer solution (30 mM Tris-HCl, 30 mM NaCl, pH 9.0) with an increasing concentration of **2** in the range of (a) 455-755 nm and (b) 570-980 nm with normalization at 650 nm. Concentration of PE-SO_3^- was 45 μM. Excitation was at 371 nm. Inset: Plot of relative emission intensity at 535 nm and 795 nm versus concentration of **2**.

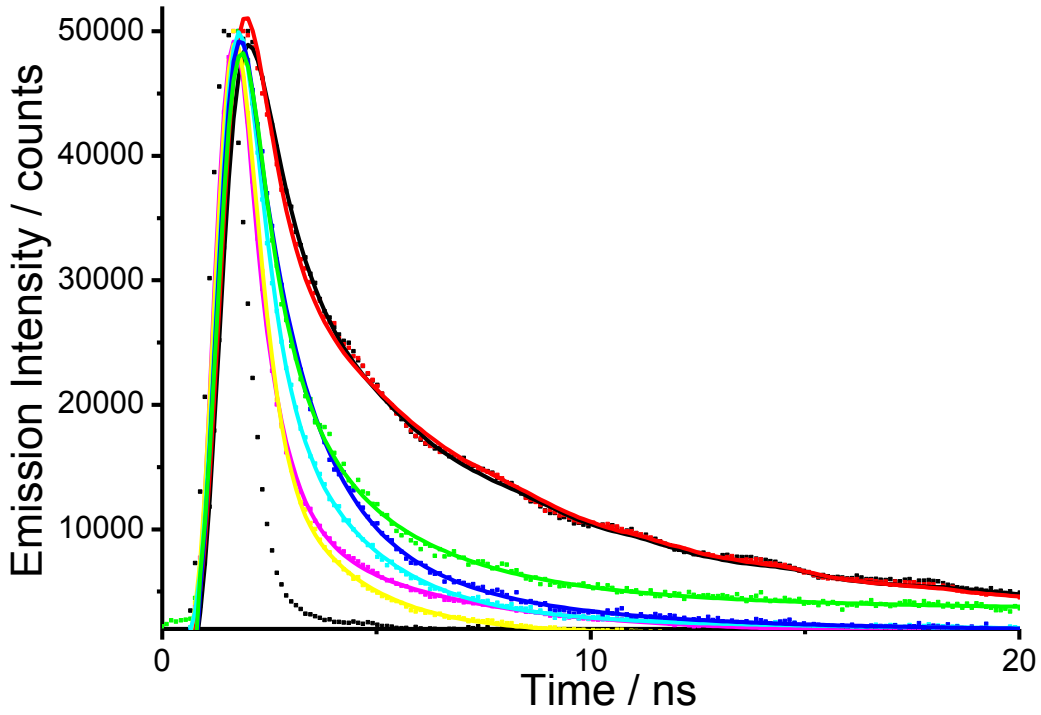

Fig. S4 Time-resolved emission decay of PPE-SO_3^- in an aqueous buffer solution (30 mM Tris-HCl, 30 mM NaCl, pH 9.0) with the concentration of **2** equal to 0 μM (black), 7.5 μM (red), 15 μM (green), 22.5 μM (blue), 30 μM (cyan), 37.5 μM (magenta) and 45 μM (yellow). Concentration of PE-SO_3^- was 45 μM. Excitation was at 371 nm and emission signals were monitored at 535 nm. The prompt signal is shown in black squares without any line fitting.

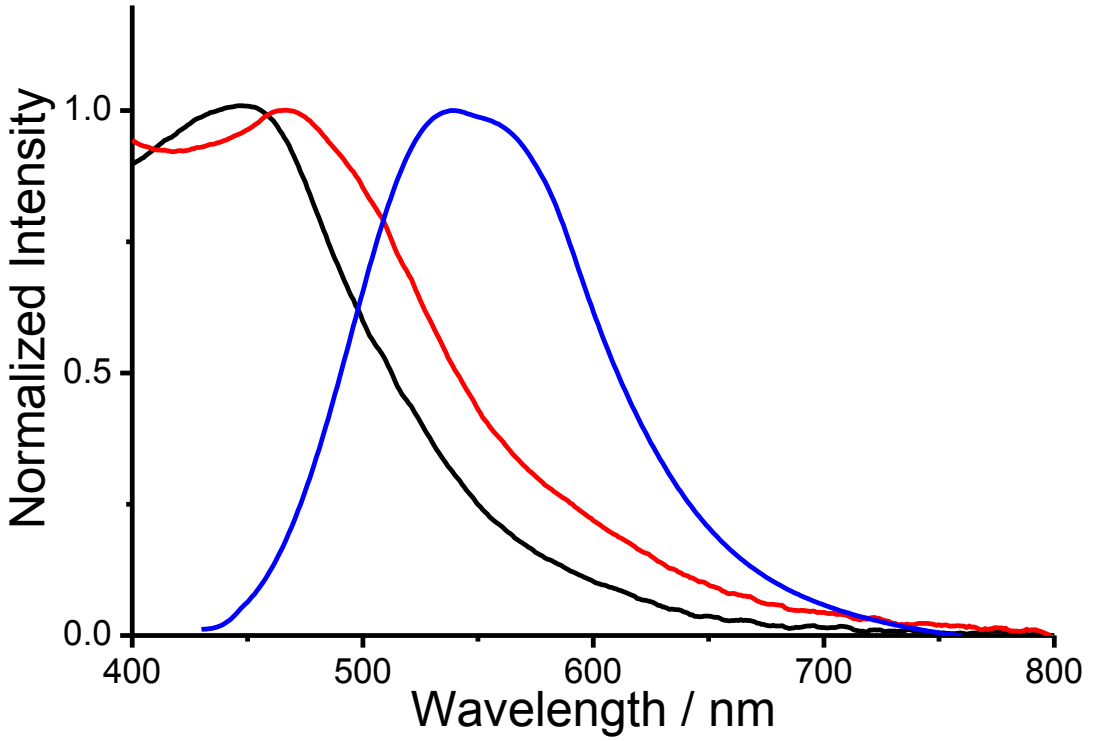

Fig. S5 Normalized electronic absorption spectra of **2** and the emission spectrum of PPE-SO_3^- showing the spectral overlap between the electronic absorption spectra of **2** with the emission spectrum of PPE-SO_3^-. The black and red lines represent the electronic absorption spectra of **2** in the absence of polyelectrolyte and in the presence of poly(sodium *p*-styrenesulfonate) with 45 μM sulfonate concentration normalized at 448 and 468 nm respectively, while the blue line represents the emission spectrum of PPE-SO_3^- with 45 μM of PE-SO_3^- normalized at 535 nm. All the spectra were recorded in an aqueous buffer solution (30 mM Tris-HCl, 30 mM NaCl, pH 9.0). Electronic absorption spectrum of the aggregated **2** was recorded using poly(sodium *p*-styrenesulfonate) instead of PPE-SO_3^-, in order to prevent the interference of the electronic absorption of **2** by the conjugated polymer.

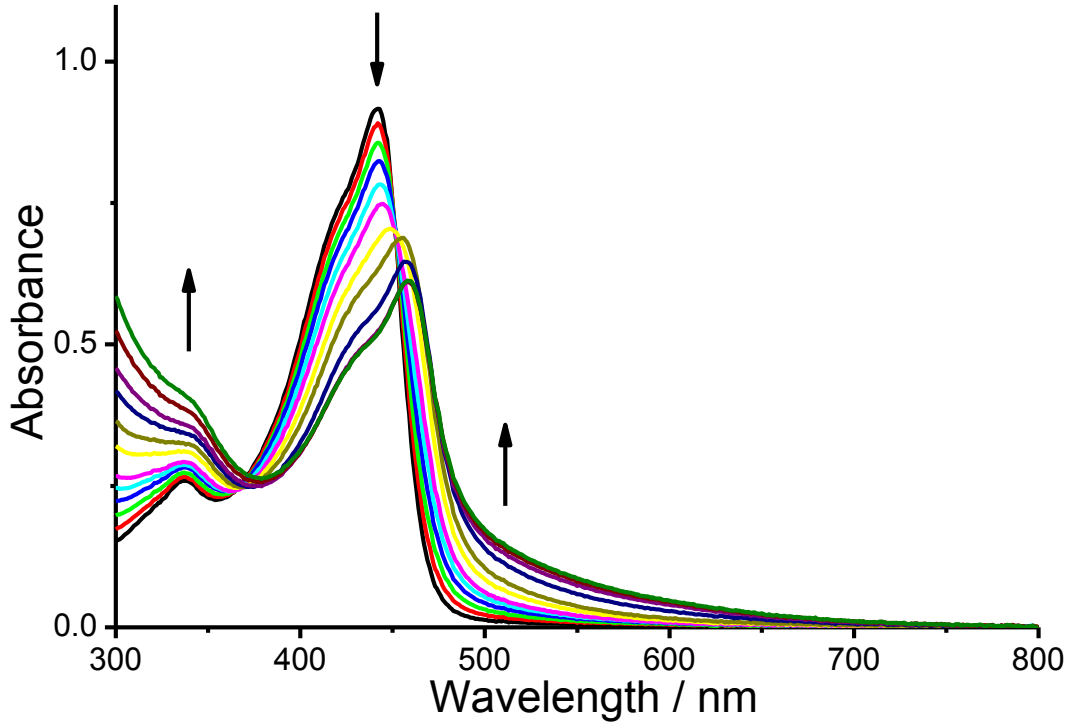

Fig. S6 Electronic absorption spectral changes of PPE-SO_3^- in an aqueous buffer solution (30 mM Tris-HCl, 30 mM NaCl, pH 9.0) with an increasing concentration of **3**. Concentration of PE-SO_3^- was 45 μM and that of **3** was 0 μM (black), 1.5 μM (red), 3 μM (green), 4.5 μM (blue), 6 μM (cyan), 7.5 μM (magenta), 11.25 μM (yellow), 15 μM (dark yellow), 22.5 μM (navy), 30 μM (purple), 37.5 μM (wine) and 45 μM (olive) respectively.

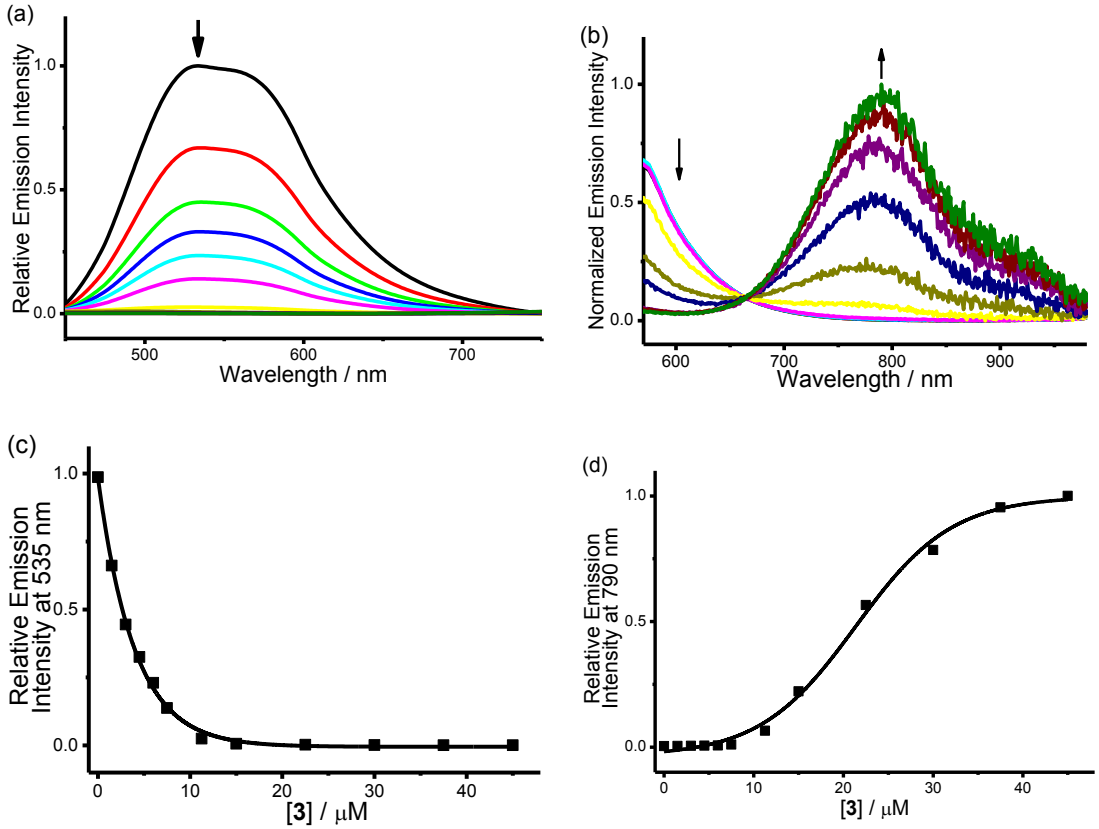

Fig. S7 Emission spectral changes of PPE-SO_3^- in an aqueous buffer solution (30 mM Tris-HCl, 30 mM NaCl, pH 9.0) with an increasing concentration of **3** in the range of (a) 450-750 nm and (b) 570-980 nm with normalization at 660 nm. Concentration of PE-SO_3^- was 45 μM. Excitation was at 369 nm. (c) Plot of relative emission intensity at 535 nm versus concentration of **3**. (d) Plot of relative emission intensity at 790 nm versus concentration of **3**.

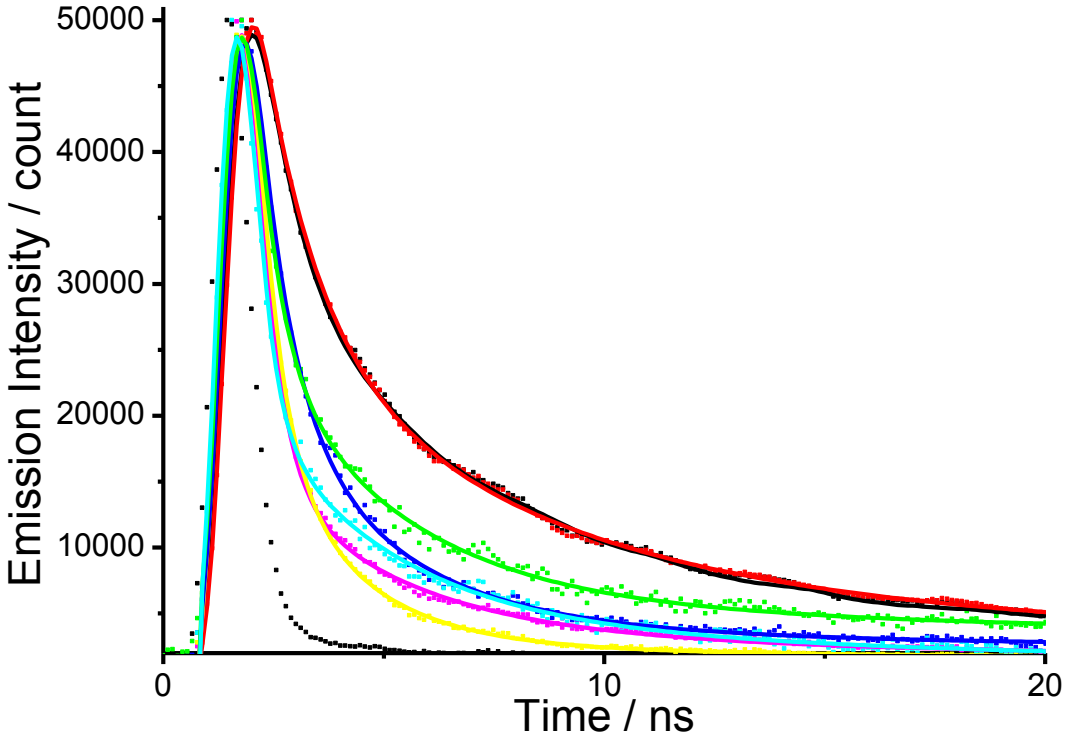

Fig. S8 Time-resolved emission decay of PPE-SO_3^- in an aqueous buffer solution (30 mM Tris-HCl, 30 mM NaCl, pH 9.0) with the concentration of **3** equal to 0 μM (black), 7.5 μM (red), 15 μM (green), 22.5 μM (blue), 30 μM (cyan), 37.5 μM (magenta) and 45 μM (yellow). Concentration of PE-SO_3^- was 45 μM. Excitation was at 371 nm and emission signals were monitored at 535 nm. The prompt signal is shown in black squares without any line fitting.

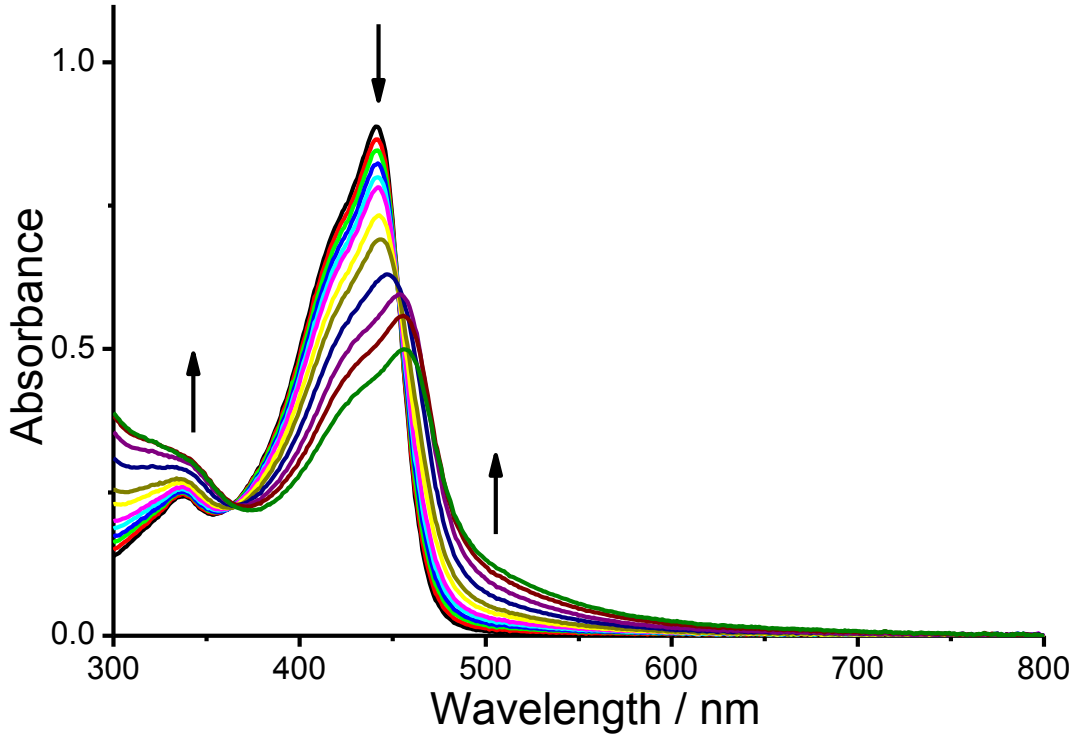

Fig. S9 Electronic absorption spectral changes of PPE-SO_3^- in an aqueous buffer solution (30 mM Tris-HCl, 30 mM NaCl, pH 9.0) with an increasing concentration of **4**. Concentration of PE-SO_3^- was 45 μM and that of **4** was 0 μM (black), 1.5 μM (red), 3 μM (green), 4.5 μM (blue), 6 μM (cyan), 7.5 μM (magenta), 11.25 μM (yellow), 15 μM (dark yellow), 22.5 μM (navy), 30 μM (purple), 37.5 μM (wine) and 45 μM (olive) respectively.

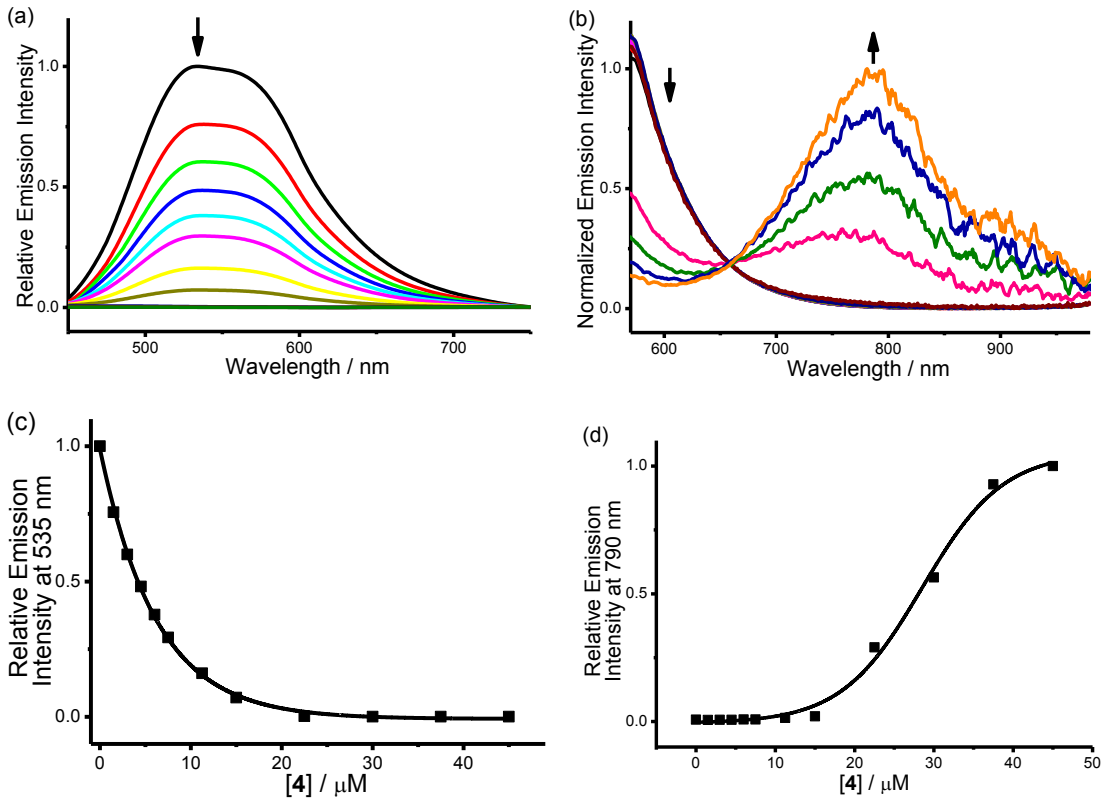

Fig. S10 Emission spectral changes of PPE-SO_3^- in an aqueous buffer solution (30 mM Tris-HCl, 30 mM NaCl, pH 9.0) with an increasing concentration of **4** in the range of (a) 450-750 nm and (b) 570-980 nm with normalization at 660 nm. Concentration of PE-SO_3^- was 45 μM. Excitation was at 364 nm. (c) Plot of relative emission intensity at 535 nm versus concentration of **4**. (d) Plot of relative emission intensity at 790 nm versus concentration of **4**.

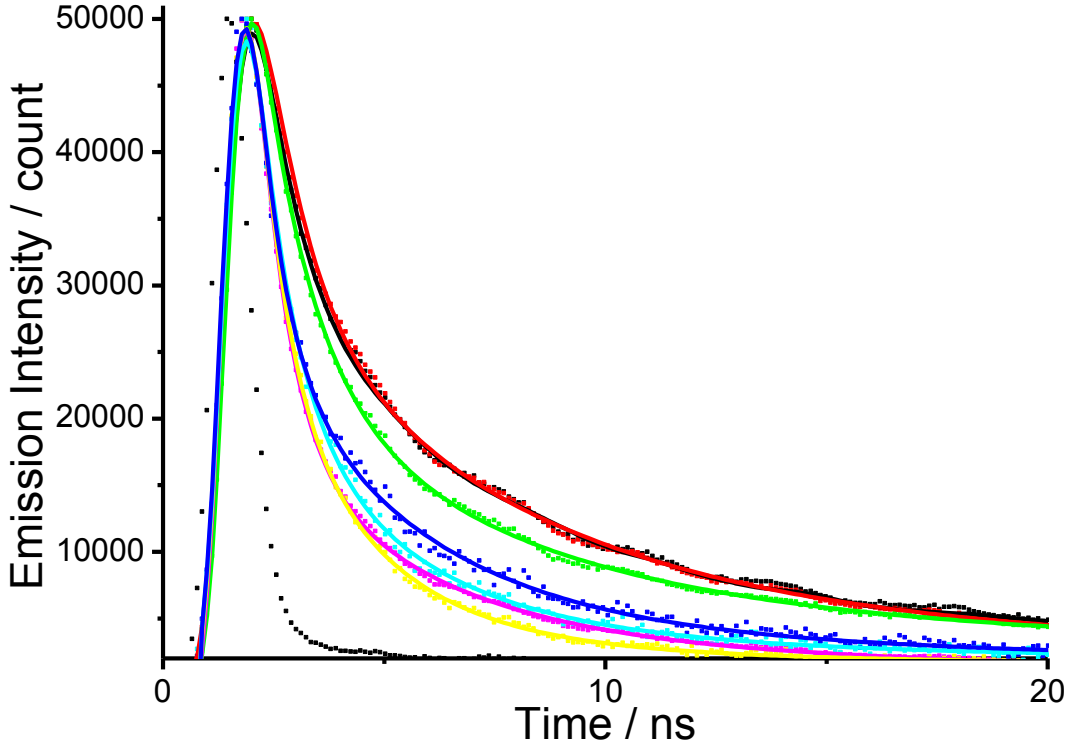

Fig. S11 Time-resolved emission decay of PPE-SO_3^- in an aqueous buffer solution (30 mM Tris-HCl, 30 mM NaCl, pH 9.0) with the concentration of **4** equal to 0 μM (black), 7.5 μM (red), 15 μM (green), 22.5 μM (blue), 30 μM (cyan), 37.5 μM (magenta) and 45 μM (yellow). Concentration of PE-SO_3^- was 45 μM. Excitation was at 371 nm and emission signals were monitored at 535 nm. The prompt signal is shown in black squares without any line fitting.

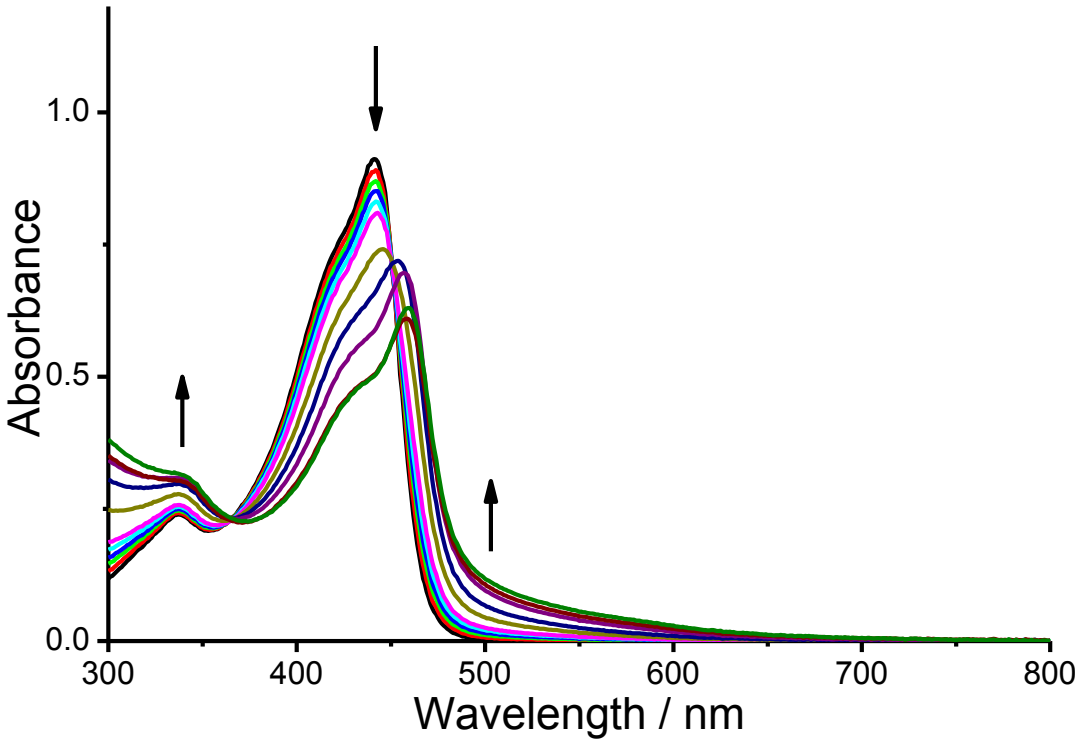

Fig. S12 Electronic absorption spectral changes of PPE-SO_3^- in an aqueous buffer solution (30 mM Tris-HCl, 30 mM NaCl, pH 9.0) with an increasing concentration of **5**. Concentration of PE-SO_3^- was 45 μM and that of **5** was 0 μM (black), 1.5 μM (red), 3 μM (green), 4.5 μM (blue), 6 μM (cyan), 7.5 μM (magenta), 15 μM (dark yellow), 22.5 μM (navy), 30 μM (purple), 37.5 μM (wine) and 45 μM (olive) respectively.

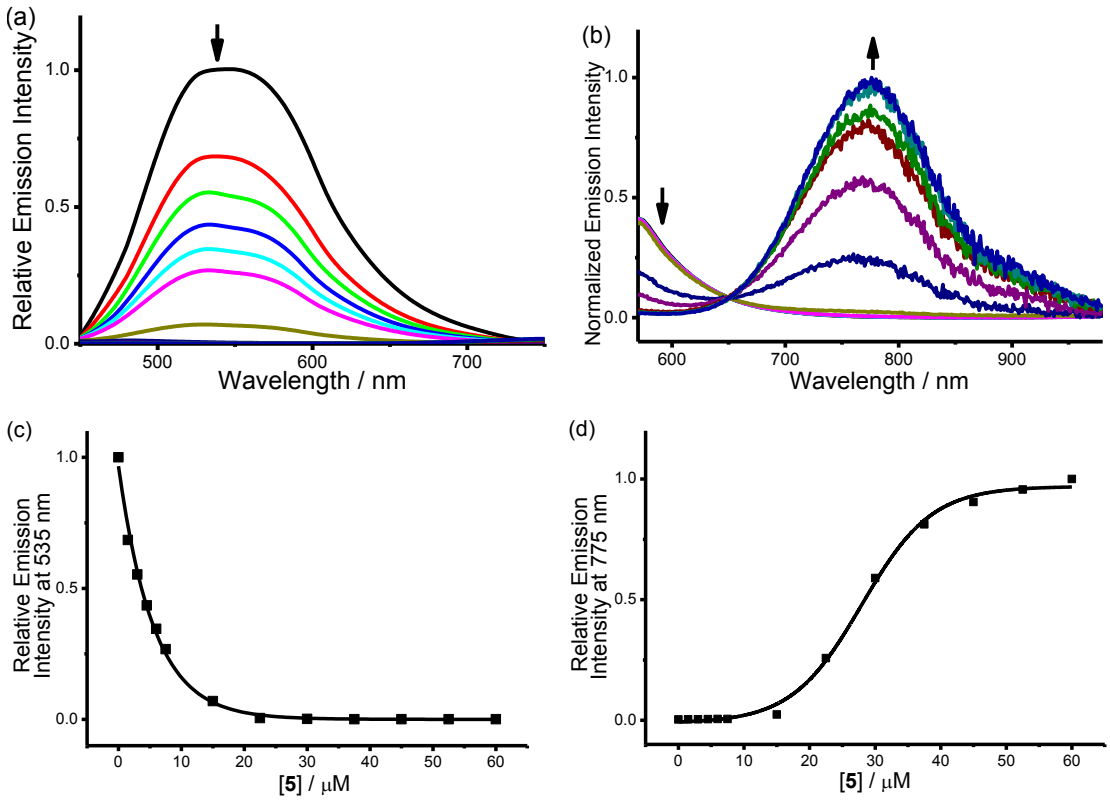

Fig. S13 Emission spectral changes of PPE-SO_3^- in an aqueous buffer solution (30 mM Tris-HCl, 30 mM NaCl, pH 9.0) with an increasing concentration of **5** in the range of (a) 450-750 nm and (b) 570-980 nm with normalization at 620 nm. Concentration of PE-SO_3^- was 45 μM. Excitation was at 365 nm. (c) Plot of relative emission intensity at 535 nm versus concentration of **5**. (d) Plot of relative emission intensity at 775 nm versus concentration of **5**.

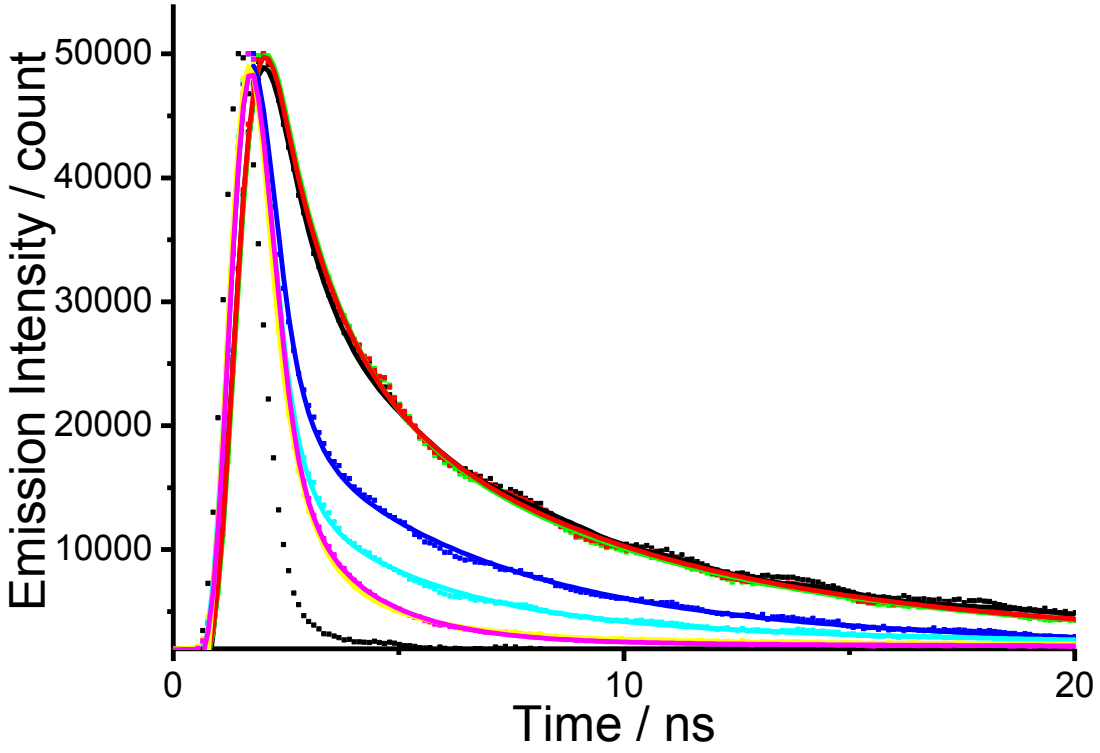

Fig. S14 Time-resolved emission decay of PPE-SO_3^- in aqueous buffer solution (30 mM Tris-HCl, 30 mM NaCl, pH 9.0) with the concentration of **5** equal to 0 μM (black), 7.5 μM (red), 15 μM (green), 22.5 μM (blue), 30 μM (cyan), 37.5 μM (magenta) and 45 μM (yellow). Concentration of PE-SO_3^- was 45 μM. Excitation was at 371 nm and emission signals were monitored at 535 nm. The prompt signal is shown in black squares without any line fitting.

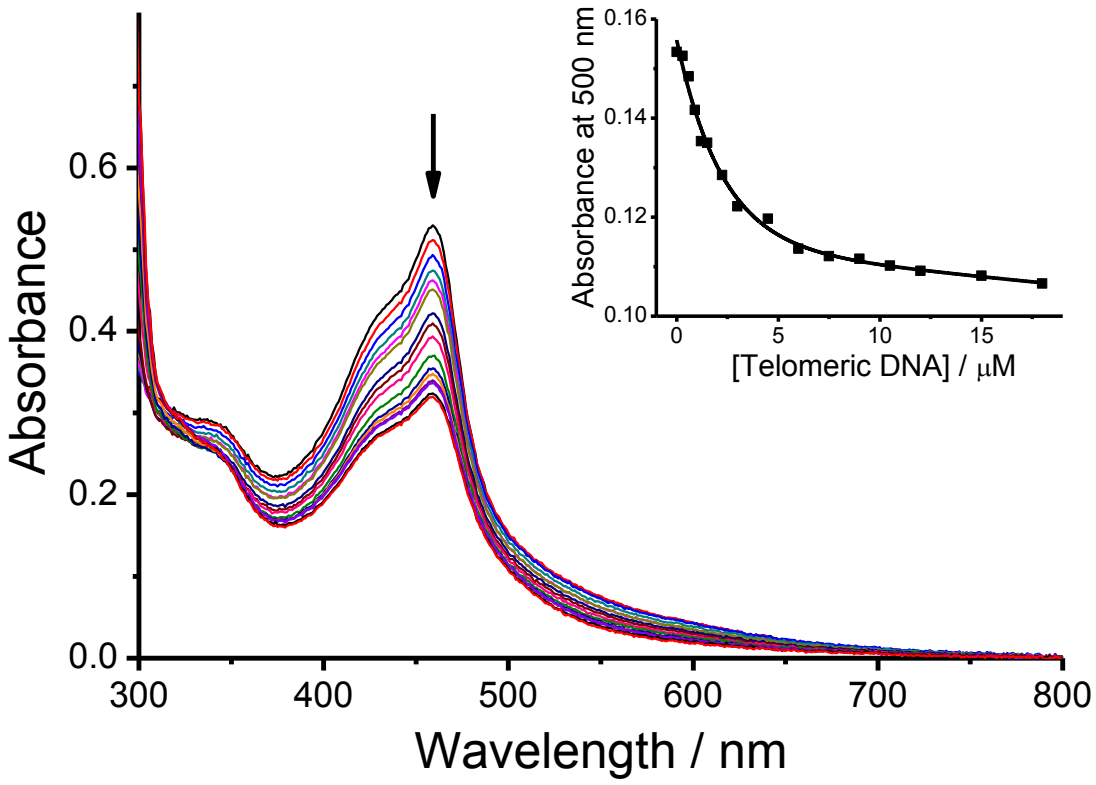

Fig. S15 Electronic absorption spectral changes of PPE-SO_3^- and **2** with an increasing concentration of human telomeric DNA in pH 6.8 aqueous buffer solution (50 mM KH_2PO_4). Concentration of PE-SO_3^- and **2** in the final solution mixture were both 45 μM. Inset: Plot of absorbance at 500 nm versus concentration of human telomeric DNA.

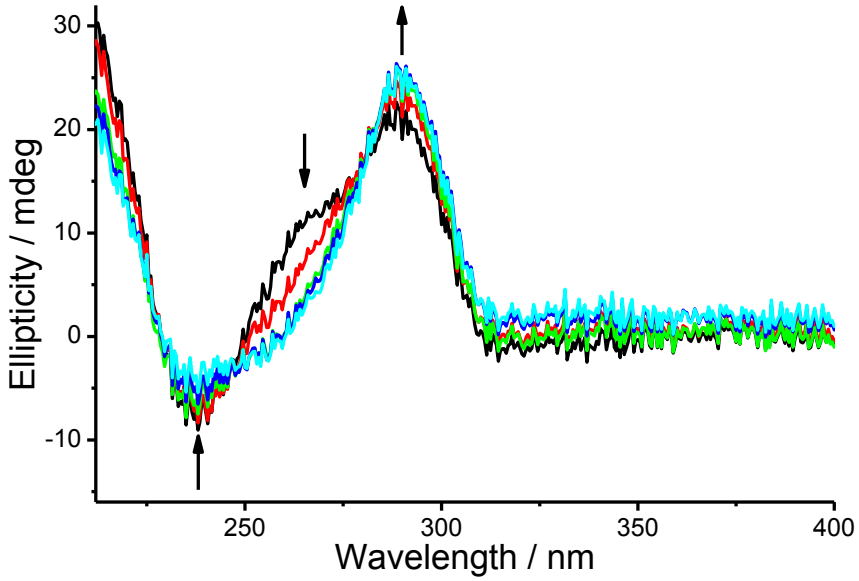

Fig. S16 CD spectra of human telomeric DNA (4 μM) in an aqueous buffer solution (50 mM KH_2PO_4, pH 6.8) with 0 μM (black), 1 μM (red), 3 μM (green), 6 μM (blue) and 8 μM (cyan) of complex **2**.

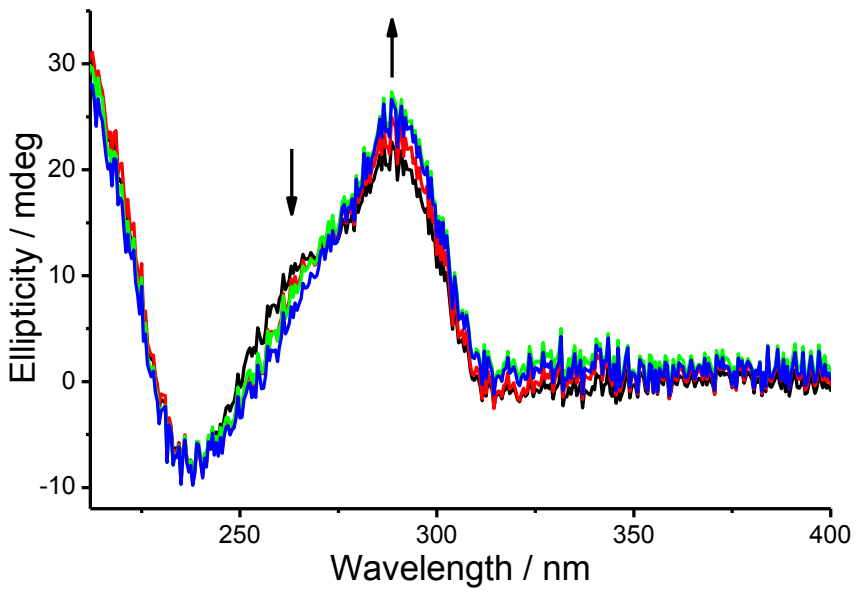

Fig. S17 CD spectra of human telomeric DNA (4 μM) in an aqueous buffer solution (50 mM KH_2PO_4, pH 6.8) with different concentrations of PPE-SO_3^-. The concentration of PE-SO_3^- was 0 μM (black), 1 μM (red), 2 μM (green) and 3 μM (blue) respectively.

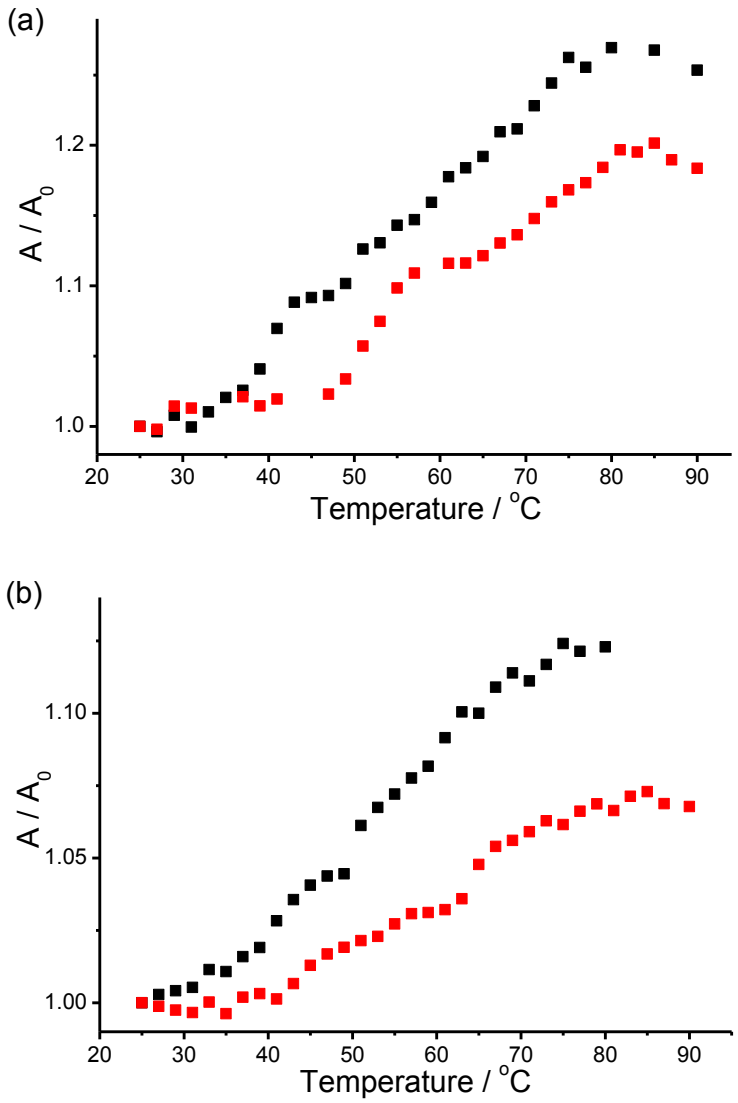

Fig. S18 UV melting curves of the human telomeric DNA (4 μM) in the aqueous buffer solution (50 mM KH_2PO_4, pH 6.8) in the absence (black) and in the presence (red) of the PPE-SO_3^-–**2** ensemble (Concentration of PE-SO_3^- and **2** in the final solution mixture were both 30 μM). A_0 and A are the absorbance at the monitored wavelength at 25 °C and at different temperatures respectively. The absorption changes were monitored at (a) 212 nm and (b) 258 nm, which are the isosbestic point in the absorption spectra of the ensemble at different temperatures and the selected wavelength for UV melting study commonly employed in the literature, respectively.

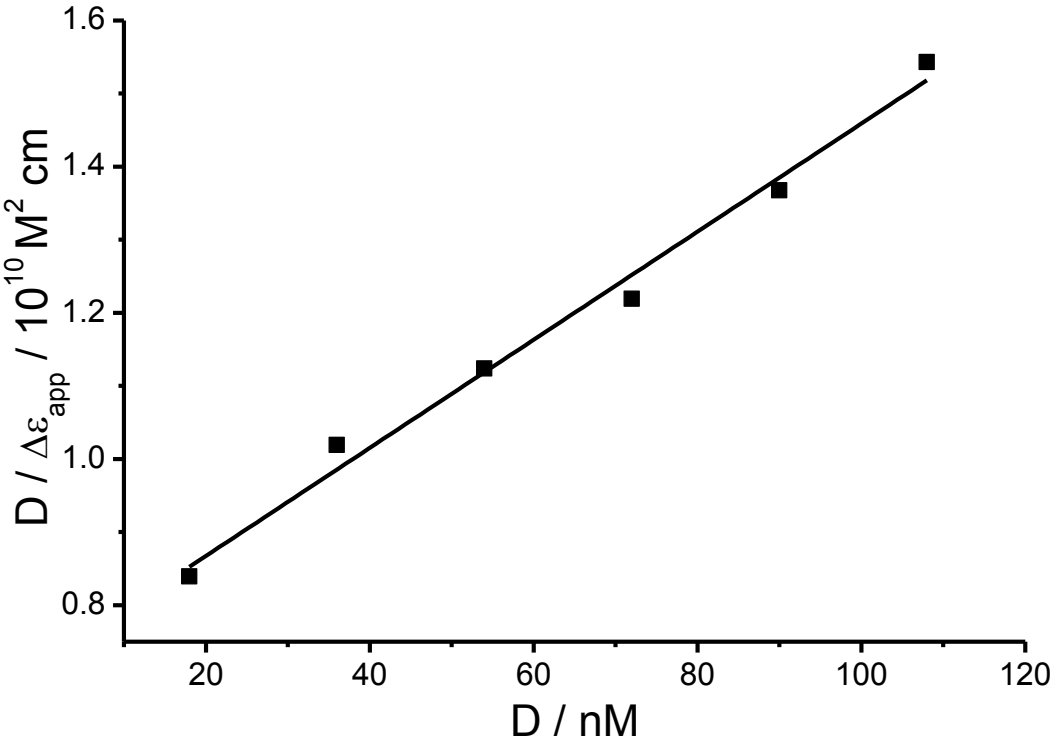

Fig. S19 A plot of $D/\Delta\varepsilon_{app}$ against D for the determination of the binding constant of complex **2** with human telomeric DNA. D is the concentration of the base pairs of human telomeric DNA and $\Delta\varepsilon_{app} = [\varepsilon_A - \varepsilon_F]$, where ε_A is calculated from the observed absorbance at 462 nm divided by the concentration of complex **2** (45 μM) and ε_F is the molar extinction coefficient of unbound complex **2** at 462 nm.

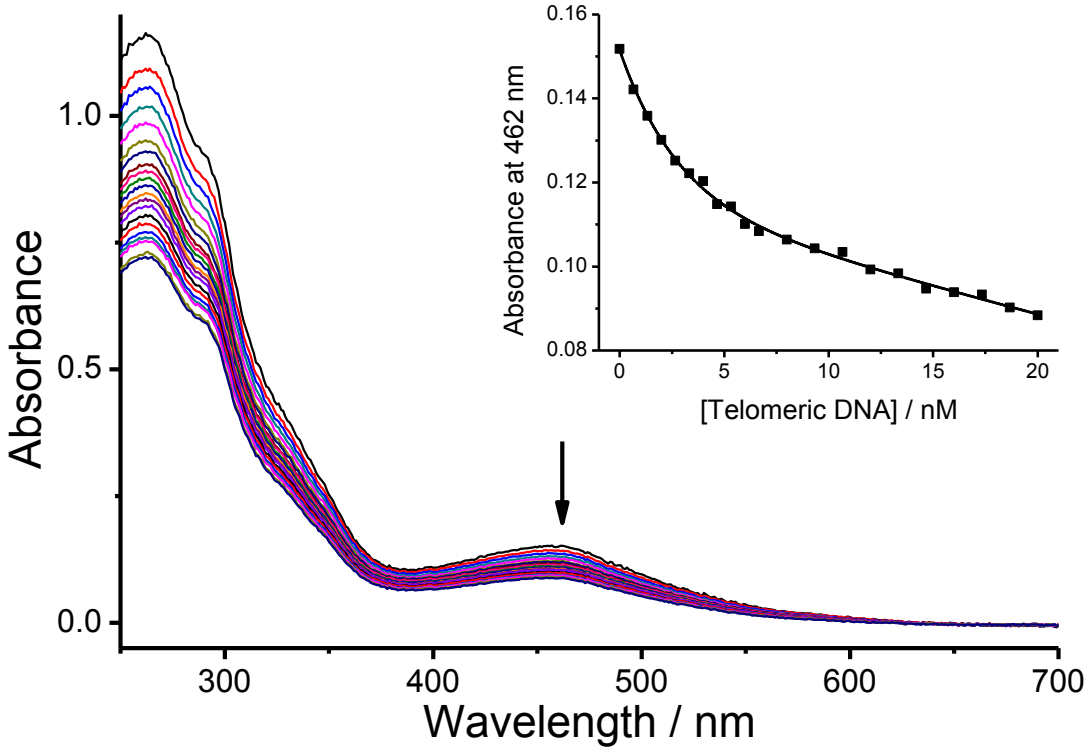

Fig. S20 Electronic absorption spectral changes of complex **2** with an increasing concentration of human telomeric DNA in pH 6.8 aqueous buffer solution (50 mM KH_2PO_4). Concentration of **2** in the final solution mixture was 45 μM. Inset: Plot of absorbance at 462 nm versus concentration of human telomeric DNA.

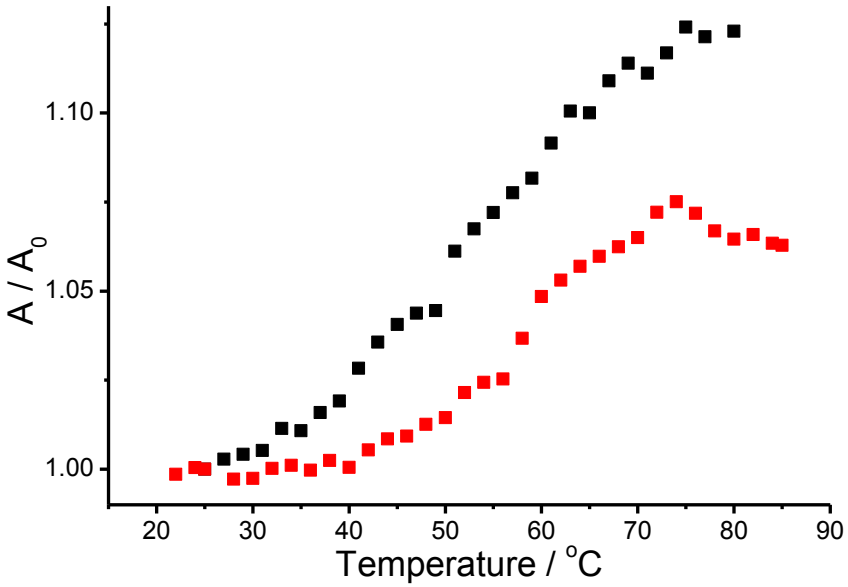

Fig. S21 UV melting curves of the human telomeric DNA (4 μM) in the aqueous buffer solution (50 mM KH_2PO_4, pH 6.8) in the absence (black) and in the presence (red) of complex **2** (concentration of **2** in the final solution mixture was 4 μM). A_0 and A are the absorbance at the 258 nm at 25 °C and at different temperatures respectively. The absorption change was monitored at 258 nm, which is commonly employed in the literature for UV melting study.

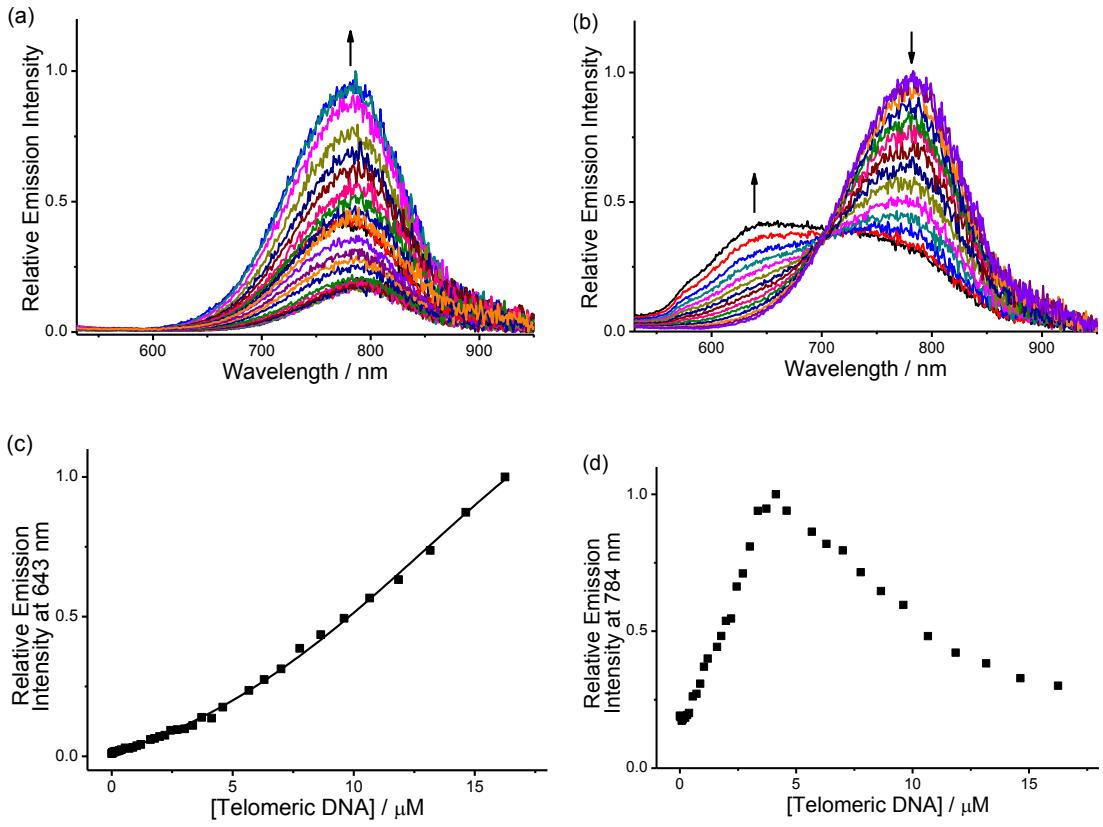

Fig. S22 Emission spectral changes of complex **2** in the aqueous buffer solution (50 mM KH_2PO_4, pH 6.8) with (a) 0−4.13 μM and (b) 4.13−16.25 μM of human telomeric DNA. Excitation was at 371 nm. (c) Plot of relative emission intensity at 643 nm versus concentration of human telomeric DNA. (d) Plot of relative emission intensity at 784 nm versus concentration of human telomeric DNA.

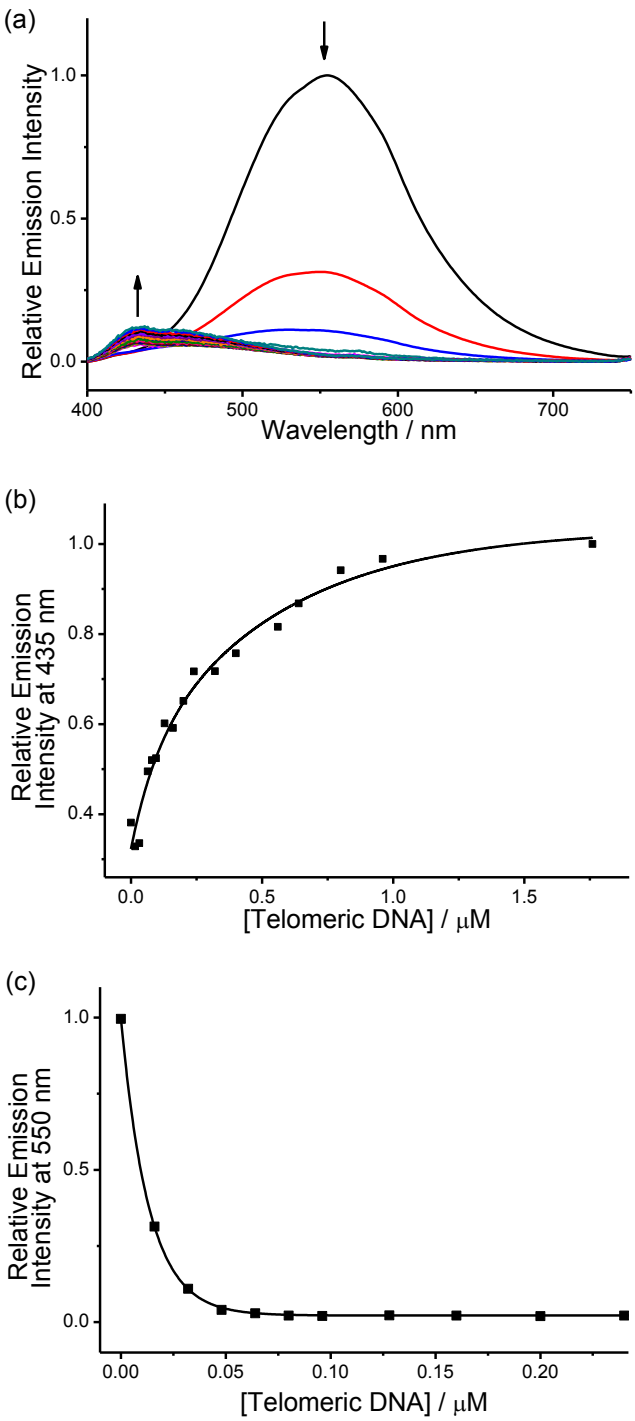

Fig. S23 (a) Emission spectral changes of PPE-SO_3^- in the aqueous buffer solution (50 mM KH_2PO_4, pH 6.8) with an increasing concentration of human telomeric DNA. Concentration of PE-SO_3^- was 45 μM. Plots of relative emission intensity of PPE-SO_3^- centered at (b) 435 nm and (c) 550 nm respectively.

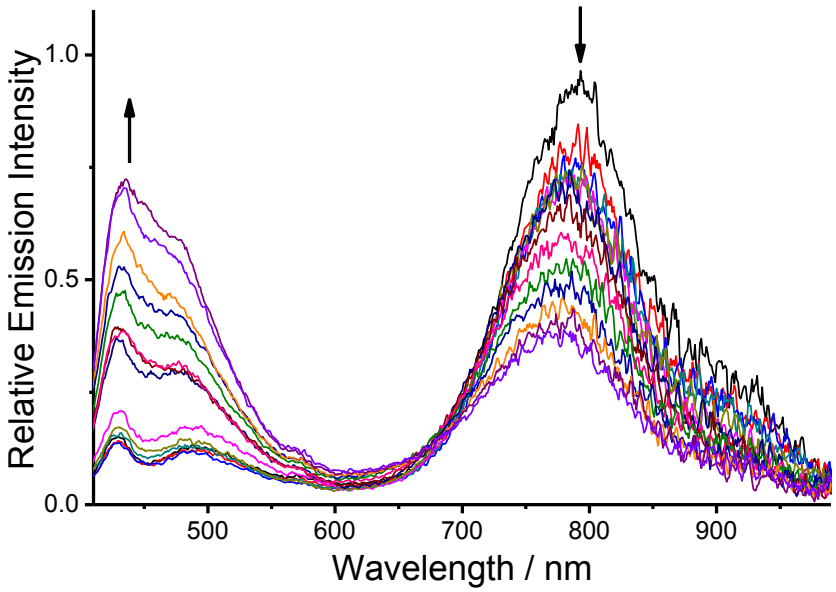

Fig. S24 Emission spectral changes of PPE-SO_3^- and **2** with an increasing concentration of *bcl-2* (0 μM – 10 μM) in pH 6.8 aqueous buffer solution (50 mM KH_2PO_4). Concentration of PE-SO_3^- and **2** in the final solution mixture were both 45 μM. Excitation was at 371 nm.

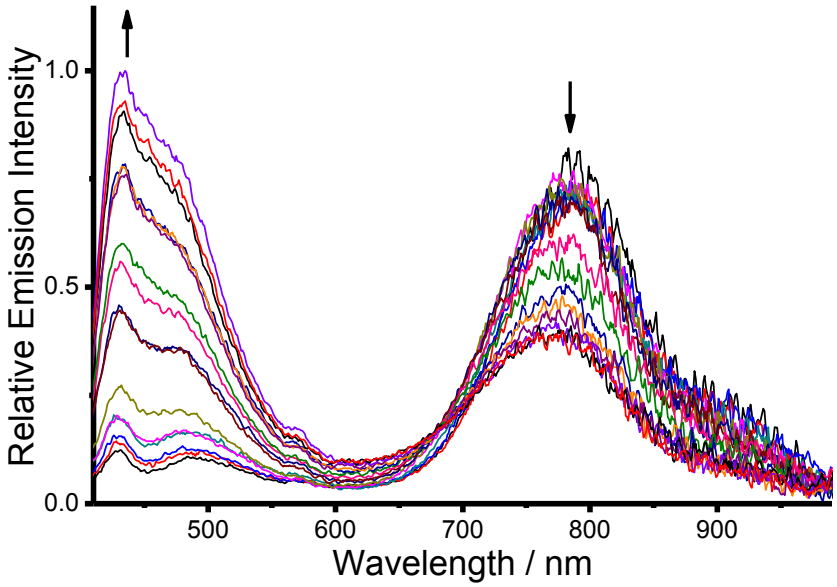

Fig. S25 Emission spectral changes of PPE-SO_3^- and **2** with an increasing concentration of *c-kit* (0 μM – 10 μM) in pH 6.8 aqueous buffer solution (50 mM KH_2PO_4). Concentration of PE-SO_3^- and **2** in the final solution mixture were both 45 μM. Excitation was at 371 nm.

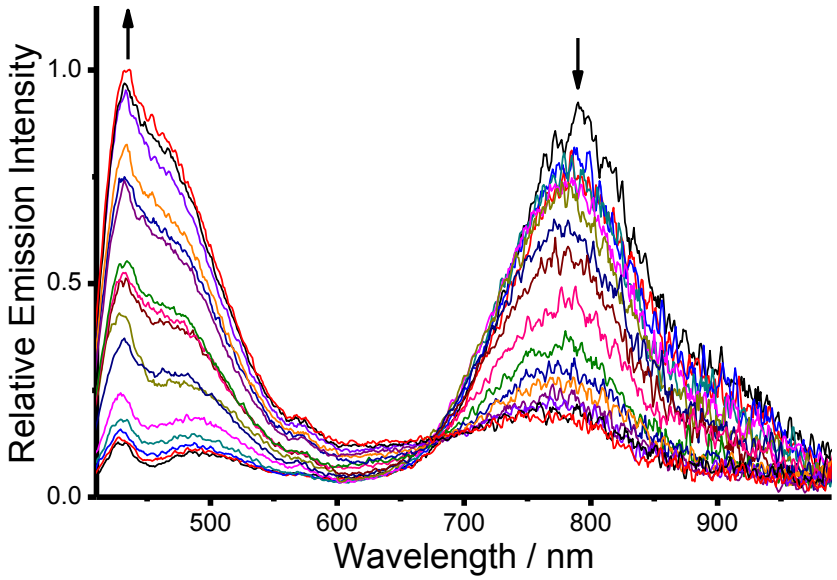

Fig. S26 Emission spectral changes of PPE-SO_3^- and **2** with an increasing concentration of *c-myc* (0 μM – 10 μM) in pH 6.8 aqueous buffer solution (50 mM KH_2PO_4). Concentration of PE-SO_3^- and **2** in the final solution mixture were both 45 μM. Excitation was at 371 nm.

Table S1 Parameters obtained from the time-resolved emission experiments of PPE-SO_3^- in an aqueous buffer solution (30 mM Tris-HCl, 30 mM NaCl, pH 9.0) with different concentrations of **1**-**5**.

Complex	Concentration[a] / μM	τ_1[b] / ns	τ_2[b] / ns
1	0	1.64 (32 %)	7.48 (68 %)
	7.5	1.52 (32 %)	7.08 (68 %)
	15	1.07 (42 %)	4.74 (58 %)
	22.5	0.88 (37 %)	4.05 (63 %)
	30	0.74 (50 %)	3.54 (50 %)
	37.5	0.70 (62 %)	3.10 (38 %)
	45	0.64 (65 %)	2.83 (35 %)
2	0	1.64 (32 %)	7.48 (68 %)
	7.5	1.52 (35 %)	7.06 (65 %)
	15	1.05 (53 %)	5.13 (46 %)
	22.5	0.82 (50 %)	4.78 (50 %)
	30	0.70 (47 %)	3.56 (53 %)
	37.5	0.55 (32 %)	3.36 (68 %)
	45	0.40 (32 %)	2.67 (68 %)
3	0	1.64 (32 %)	7.48 (68 %)
	7.5	1.52 (26 %)	7.37 (74 %)
	15	1.05 (43 %)	6.43 (57 %)
	22.5	0.96 (50 %)	5.75 (50 %)
	30	0.78 (42 %)	5.53 (58 %)
	37.5	0.56 (48 %)	4.01 (52 %)
	45	0.52 (58 %)	3.82 (42 %)
4	0	1.64 (32 %)	7.48 (68 %)
	7.5	1.52 (30 %)	7.37 (70 %)
	15	1.23 (31 %)	6.97 (69 %)
	22.5	1.08 (37 %)	5.17 (63 %)
	30	0.96 (44 %)	4.70 (56 %)
	37.5	0.79 (41 %)	4.48 (59 %)
	45	0.71 (46 %)	4.20 (54 %)
5	0	1.64 (32 %)	7.48 (68 %)
	7.5	1.43 (25 %)	7.20 (75 %)
	15	1.13 (20%)	6.88 (80 %)
	22.5	0.64 (32 %)	5.61 (68 %)
	30	0.61 (50 %)	4.10 (50 %)

	37.5	0.61 (70 %)	3.11 (30 %)
	45	0.58 (70 %)	3.06 (30 %)

[a] The concentration of PE-SO_3^- was 45 μM.

[b] τ_1 and τ_2 are the lifetimes of the biexponential decay.

Table S2 UV melting temperatures of the G-quadruplex DNAs, T_m, in the absence and in the presence of complex **2**.

G-quadruplex DNA[a]	T_m in the absence of **2** / °C	T_m in the presence of **2**[b] / °C
Human telomeric DNA[c]	51	58
bcl-2[d]	68	72
c-kit[d]	56	64
c-myc[d]	74	82

[a] The concentration of G-quadruplex DNAs was 4 μM.

[b] The concentration of complex **2** was 4 μM.

[c] The UV−vis absorption changes were monitored at 258 nm.

[d] The UV−vis absorption changes were monitored at 216 nm.

References:

S1 J. Wang and G. S. Hanan, *Synlett*, 2005, **8**, 1251.

S2 J. M. Haider, M. Chavarot, S. Weidner, I. Sadler, R. M. Williams, L. D. Cola and Z. Pikramenou, *Inorg. Chem.*, 2001, **40**, 3912.

S3 A. Elangovan, S. W. Yang, J. H. Lin, K. M. Kao and T. I. Ho, *Org. Biomol. Chem.*, 2004, **2**, 1597.

S4 C. Gottardo and A. Aguirre, *Tetrahedron Lett*., 2002, **43**, 7091.

S5 J. Chen, J. W. Kampf and A. J. McNeil, *Langmuir*, 2010, **26**, 13076.

S6 (a) C. Tan, M. R. Pinto and K. S. Schanze, *Chem. Commun.*, 2002, 446; (b) S. A. Kushon, K. D. Ley, K. Bradford, R. M. Jones, D. McBranch and D. Whitten, *Langmuir*, 2002, **18**, 7274.

S7 J. T. Wang, Y. Li, J. H. Tan, L. N. Ji, Z. W. Mao, *Dalton Trans.*, 2011, **40**, 564.

S8 (a) G. T. Morgan and F. H. Burstall, *J. Chem. Soc.*, 1934, 1498; (b) M. Howe-Grant and S. J. Lippard, *Inorg. Synth.*, 1980, **20**, 101; (c) J. A. Bailey, M. G. Hill, R. E. Marsh, V. M. Miskowski, W. P. Schaefer and H. B. Gray, *Inorg. Chem.*, 1995, **34**, 4591.

S9 (a) C. Yu, K. H. Y. Chan, K. M. C. Wong and V. W. W. Yam, *Chem.–Eur. J.*, 2008, **14**, 4577; (b) C. Y. S. Chung, K. H. Y. Chan, and V. W. W. Yam, *Chem. Commun.*, 2011, **47**, 2000; (c) C. Y. S. Chung and V. W. W. Yam, *J. Am. Chem. Soc.*, 2011, **133**, 18775.

S10 (a) V. W. W. Yam, R. P. L. Tang, K. M. C. Wong and K. K. Cheung, *Organometallics*, 2001, **20**, 4476; (b) K. Sonogashira, S. Takahashi and N. Hagihara, *Macromolecules*, 1977, **10**, 879; (c) S. Takahashi, M. Kariya, T. Yakate, K. Sonogashira and N. Hagihara, *Macromolecules*, 1978, **11**, 1063.

S11 (a) M. P. Teulade-Fichou, C. Carrasco, L. Guittat, C. Bailly, P. Alberti, J. L. Mergny, A. David, J. M. Lehn and W. D. Wilson, *J. Am. Chem. Soc.*, 2003, **125**,

4732; (b) C. C. Chang, C. W. Chien, Y. H. Lin, C. C. Kang and T. C. Chang *Nucleic Acids Res.*, 2007, **35**, 2846; (c) Q. Yang, J. Xiang, S. Yang, Q. Zhou, Q. Li, Y. Tang and G. Xu, *Chem. Commun.*, 2009, 1103.

S12 (a) T. Förster, *Ann. Phys.*, 1948, **2**, 55; (b) T. Förster, *Faraday Discuss.*, 1959, **27**, 7.

S13 C. V. Kumar and E. H. Asuncion, *J. Am. Chem. Soc.*, 1993, **115**, 8541.

S14 (a) F. Koeppel, J. F. Riou, A. Laoui, P. Mailliet, P. B. Arimondo, D. Labit, O. Petitgenet, C. Hélène and J. L. Mergny, *Nucleic Acids Res.*, 2001, **29**, 1087; (b) F. X. Han, R. T. Wheelhouse and L. H. Hurley, *J. Am. Chem. Soc.*, 1999, **121**, 3563.